EOF Analysis of ENSO Variability

1. Introduction

The El Niño-Southern Oscillation (ENSO) cycle is a coupled atmospheric-oceanic climate pattern in the Equatorial Pacific Ocean and one of the most significant drivers of annual global climate variability[1]. During neutral conditions, strong easterly trade winds drive warm surface water westward along the equator, creating a warm pool in the western Pacific and upwelling cold water in the eastern Pacific[2]. El Niño events occur when the easterly trade winds weaken, allowing warm water to shift eastward[3,4]. La Niña events occur when easterly winds strengthen, intensifying the normal temperature gradient[5]. Sea surface temperature is linked to atmospheric pressure and wind velocity through Walker Circulation, which drives atmospheric overturning in the Pacific[6].

Empirical Orthogonal Function (EOF) analyses are performed to understand the relative spatiotemporal significance of atmospheric-oceanic anomalies characteristic of ENSO events. EOF analyses produce multiple modes of variability: each mode has an *eigenvalue* - the proportion of variance explained by the EOF mode; and an *eigenvector* containing the spatial structure of variability given by the mode[7]. Modes are produced in hierarchical order, such that the first mode is the most significant in explaining the data variance. The eigenvectors are presented as *loading patterns*[7] corresponding to the *index time series* of *principal components* indicating the loading pattern's amplitude - or intensity - through time[7].

Due to the irregular duration and frequency of ENSO events, continuous assessment of evolving conditions in the Equatorial Pacific is crucial for anticipating disruptions to global weather patterns[6,7], and preparing for risks to safety, food security, water resources, and infrastructure[8,9].

2. Methods

Global measurements between 1979-2017 for four variables - mean atmospheric pressure at sea level (msl), sea surface temperature (sst), and zonal (latitudinal) and meridional (longitudinal) wind velocities 10m above sea level - were sourced from the ERA Interim reanalysis dataset.

To quantify the dominant mode of variability in ENSO events (EOF1), EOF analysis was done in Python using xarray datasets and the eofs.standard package's solver. The datasets were filtered for 30°S-30°N and 100°E-70°W to encompass the Pacific Ocean; spatial coordinates were flattened from two-dimensional longitude and latitude to one-dimensional space. Land coordinates were identified as null sst values, then excluded from all datasets to analyse only ocean-atmospheric processes. Rolling averages over consecutive months were calculated to obtain values for "bimonthly seasons" and labelled as new coordinates; null values (along the time dimension) were dropped. Each dataset was split up according to the bimonthly seasons and concatenated (along the spatial dimension) to the corresponding subsets of the other variables, resulting in 12 piecewise datasets containing one bimonthly season's measurements for sea coordinates of all variables. With 0s replacing remaining null data, EOF analysis was done on all 12

datasets. Each variable's EOF1 loading pattern was extracted by taking a slice of the piecewise matrix, with dimensions matching the corresponding raw un-concatenated variable matrix. Principal components were also recorded: a scaling factor of $\sqrt{\lambda}$ for eigenvalue λ, was included to ensure that the principal components (multiplicative) and loading patterns (reciprocal) had an order of 1.

3. Results

Since El Niño events typically reach peak intensity during boreal winters, the bimonthly season of December-January is analysed in this study. EOF1 for this period accounts for 17.68% of the data's variation.

Positive anomalies in the index time series (Figure 1) indicate El Niño conditions, while negative anomalies indicate La Niña conditions. Note the numerical boundaries of ENSO events are not defined here; the analysis uses positive and negative EOF values to indicate presence of characteristics associated with the ENSO event.

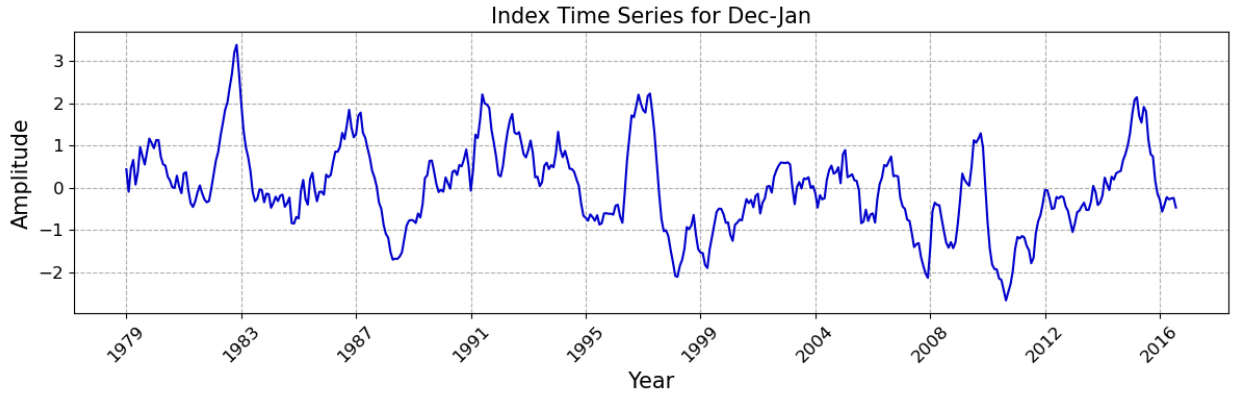

Figure 1. The Index Time Series of EOF1 presents the spatially weighted anomalies of EOF1 eigenvectors. It reflects the varying amplitude - or intensity - of the mode through the years 1979-2017. Positive anomalies in the time series indicate changes in the variables - sea surface temperature (sst), mean sea level pressure (ml), meridional wind velocity, and zonal wind velocity - associated with El Niño events, while negative anomalies indicate changes in the variables associated with La Niña events.

The loading patterns (Figures 2-5) indicate the locations with the most significant data variance. Positive loadings (red) indicate a positive relationship with EOF1 - the variable increases with an increasing EOF value, or decreases with a decreasing EOF value. In these areas, variables increase during El Niño and decrease during La Niña. Negative loading areas (blue) reflect a negative relationship with EOF1 and an opposite correlation with ENSO events. For wind velocity, an increase indicates increased northward meridional winds, and eastward zonal winds.

In Figure 5, zonal wind patterns show a decrease in westward wind velocity, reflecting a weakening/reversal of the easterly trade winds, characteristic of El Niño. This corresponds to an increase

in sst across the central and eastern Pacific and a decrease in the west (Figure 2), while msl increases in the west and decreases in the east (Figure 3). Figure 4 demonstrates an increase in converging northerly and southerly meridional winds at the equator during El Niño events. Note that the relative changes in magnitude are dependent on the prevailing wind directions of the area[10].

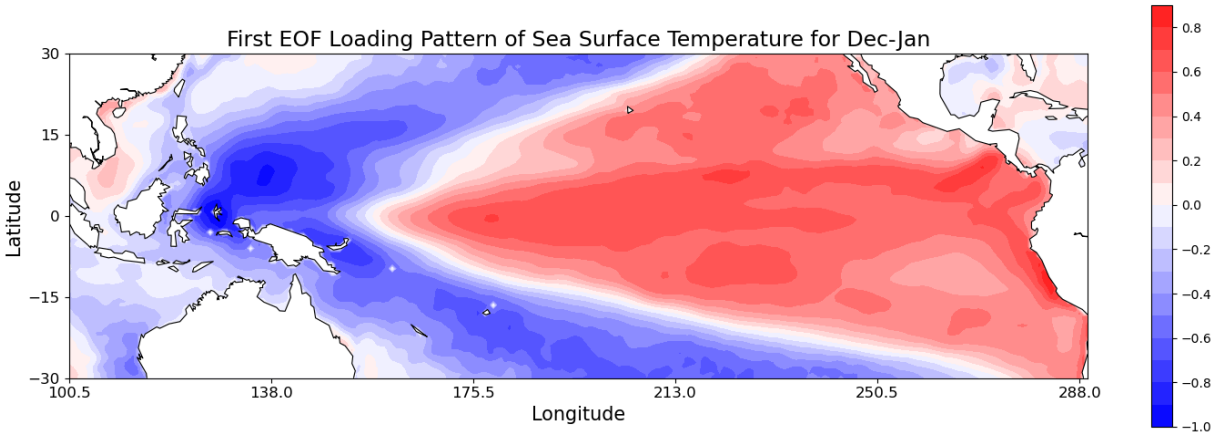

Figure 2. The EOF1 loading pattern reflects the regions most significant in determining variation of sea surface temperature (sst) for the bimonthly season December-January. The positive loading area (red) in the eastern Pacific reflects an increase in temperature during El Niño years, while the negative loading area (blue) in the western Pacific reflects a decrease in temperature during El Niño years.

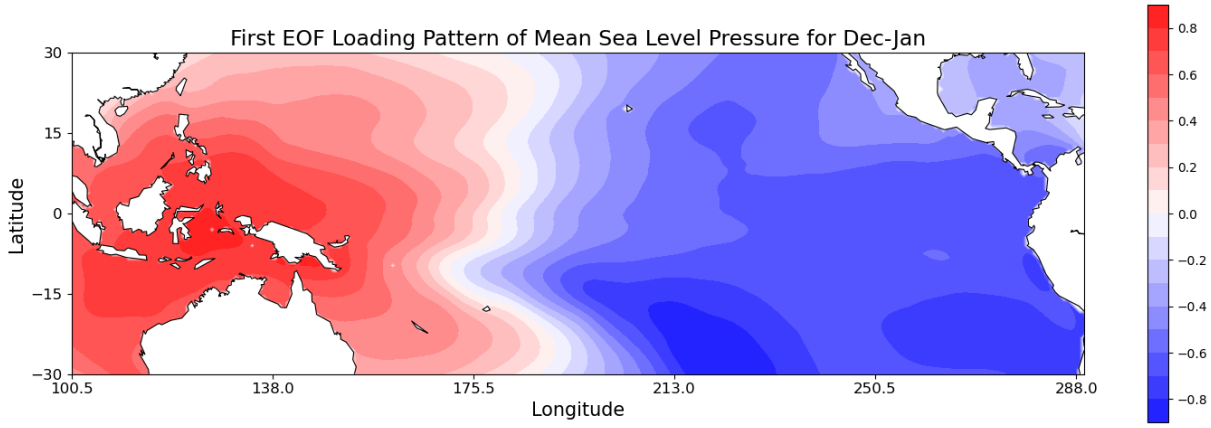

Figure 3. The EOF1 loading pattern reflects the regions most significant in determining variation of mean sea level pressure (msl) for the bimonthly season December-January. The negative loading area (blue) in the eastern Pacific reflects a decrease in atmospheric pressure during El Niño years, while the positive loading area (red) in the western Pacific reflects an increase in atmospheric pressure during El Niño years.

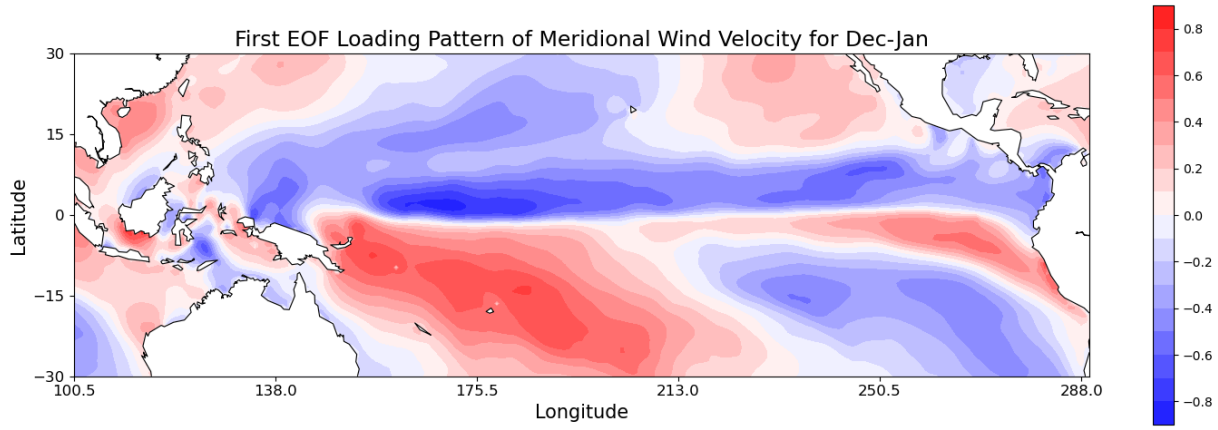

Figure 4. The EOF1 loading pattern reflects the regions most significant in determining variation of meridional (longitudinal) wind velocity (10 meters above sea level) for the bimonthly season December-January. The negative loading area (blue) in the north reflects a decrease in northward wind velocity (increase in southward wind velocity) during El Niño events, while the positive loading area (red) in the south reflects an increase in northward wind velocity during El Niño events. This pattern shows an increase in convergent wind velocities at the equator during El Niño events.

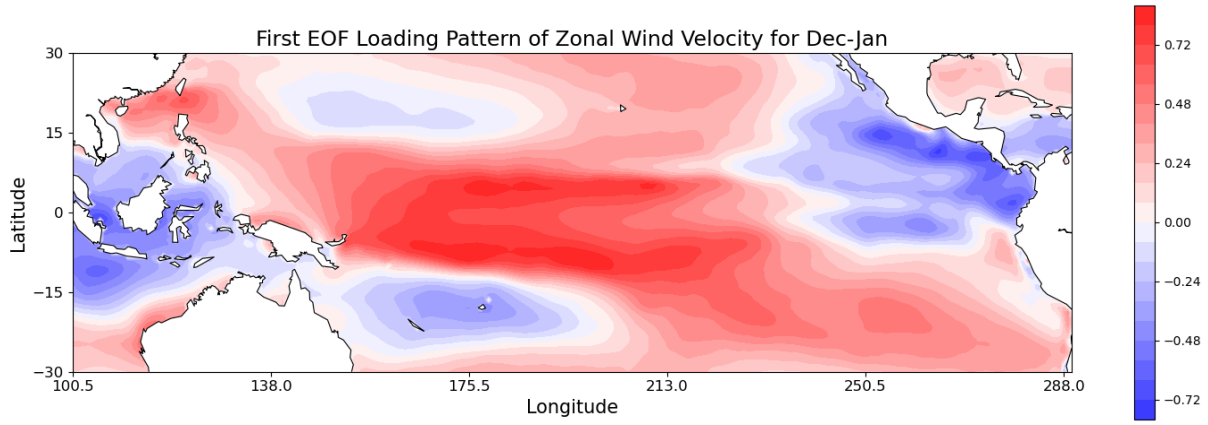

Figure 5. The EOF1 loading pattern reflects the regions most significant in determining variation of zonal (latitudinal) wind velocity (10 meters above sea level) for the bimonthly season December-January. The positive loading area (red) in the central and western Pacific reflects an increase in eastward wind velocity (decrease in westward wind velocity) during El Niño events. The positive loading area reflects a weakening or reversal of the Easterly trade winds, characteristic of an El Niño event.

4. Discussion

The driving force of El Niño is clearly exhibited in Figure 5, with weakening of easterly trade winds. This shifts the low pressure system eastward (Figure 3), causing sst increase of the eastern Pacific (Figure 2). In the equatorial Pacific, the meridional wind flows towards the equator, converging from both hemispheres. Figure 4 indicates an increase in magnitude of convergence along the equator during El

Niño events, implying amplified atmospheric convection in the Central and Eastern Pacific. This is consistent with the current understanding of El Niño's effect on Walker Circulation[6].

The trends demonstrated in this analysis align with the general characteristics associated with ENSO[11]. The results serve to reveal the spatial extent of the variable changes during both El Niño and La Niña events, highlighting potential focus areas for addressing and mitigating challenges posed by those changes.

EOF analysis is useful for identifying spatiotemporal patterns of variability, however, provides no insight into the underlying physical processes behind such variability, meaning an EOF analysis cannot be interpreted without prior knowledge of the prevailing conditions of the target region. Accuracy in our study may be improved by incorporating additional variables such as sea surface height and precipitation. Additionally, improvements may be made by broadening the analysis to investigate additional EOF modes, as the leading EOF accounts for less than 20% of variation within the data.

References

1. Mendi V, Dwarakish G. El Nino: A Review. Int J Earth Sci Eng. 2015 Apr 9;08:130–7.

2. Newman M. Winds of change. Nat Clim Change. 2013 Jun 1;3(6):538–9.

3. Anderson BT, Perez RC, Karspeck A. Triggering of El Niño onset through trade wind–induced charging of the equatorial Pacific. Geophys Res Lett. 2013 Mar 28;40(6):1212–6.

4. Yang GY, Hoskins B. ENSO Impact on Kelvin Waves and Associated Tropical Convection. J Atmospheric Sci. 2013 Nov 1;70(11):3513–32.

5. Chen N, Thual S, Stuecker MF. El Niño and the Southern Oscillation: Theory. In: Reference Module in Earth Systems and Environmental Sciences [Internet]. Elsevier; 2019. Available from: https://www.sciencedirect.com/science/article/pii/B9780124095489117658

6. Gushchina D, Zheleznova I, Osipov A, Olchev A. Effect of Various Types of ENSO Events on Moisture Conditions in the Humid and Subhumid Tropics. Atmosphere. 2020;11(12).

7. Shea D. Empirical Orthogonal Function (EOF) Analysis and Rotated EOF Analysis | Climate Data Guide [Internet]. 2023 [cited 2024 Nov 28]. Available from: https://climatedataguide.ucar.edu/climate-tools/empirical-orthogonal-function-eof-analysis-and-rotated-eof-analysis

8. Corringham TW, Cayan DR. The Effect of El Niño on Flood Damages in the Western United States. Weather Clim Soc. 2019 Jul 1;11(3):489–504.

9. World Health Organisation. El Niño Southern Oscillation (ENSO) [Internet]. 2023 [cited 2024 Nov 28]. Available from: https://www.who.int/news-room/fact-sheets/detail/el-nino-southern-oscillation-(enso)

10. Waliser DE, Jiang X. TROPICAL METEOROLOGY AND CLIMATE | Intertropical Convergence Zone. In: North GR, Pyle J, Zhang F, editors. Encyclopedia of Atmospheric Sciences (Second Edition) [Internet]. Oxford: Academic Press; 2015. p. 121–31. Available from: https://www.sciencedirect.com/science/article/pii/B9780123822253004175

11. Xu K, Tam CY, Zhu C, Liu B, Wang W. CMIP5 Projections of Two Types of El Niño and Their Related Tropical Precipitation in the Twenty-First Century. J Clim. 2017 Feb 1;30(3):849–64.